STRUCTURE AND VIBRATIONAL SPECTROSCOPIC STUDIES OF 1-NAPHTHOL: DENSITY FUNCTIONAL THEORY CALCULATIONS

Raja G.[1], Saravanan K.[2] and Sivakumar S.[3]

[1]Department of Chemistry, Paavai Engineering College, Namakkal-637 018, India
[2]Department of Chemistry, Thiruvalluvar Government Arts College, Rasipuram-637 401, India
[3]Department of Physics, Arignar Anna Government Arts College, Attur-636 121, India
Email: [1]genuineraja@gmail.com, [2]npksaran@yahoo.co.in, [3]photonic_ss@rediffmail.com

Abstract

The molecular vibrations of 1-Naphthol were investigated in polycrystalline sample, at room temperature, by FT- IR and FT-Raman spectroscopy. In parallel, ab initio and various density functional (DFT) methods were used to determine the geometrical, energetic and vibrational characteristics of 1-Naphthol. On the basis of B3LYP/6-31G* and B3LYP/6-311+G** methods and basis set combinations, a normal mode analysis was performed to assign the various fundamental frequencies according to the total energy distribution (TED). The vibrational spectra were interpreted, with the aid of normal coordinate analysis based on a scaled quantum mechanical force field. The Infrared and Raman spectra were also predicted from the calculated intensities. Comparison of simulated spectra with the experimental spectra provides important information about the ability of the computational method to describe the vibrational modes. Simulation of Infrared and Raman spectra, utilizing the results of these calculations led to excellent overall agreement with observed spectral patterns. The investigation is performed using quantum chemical calculations conducted by means of the Gaussian 98W and Guassview set of programs. Further, density functional theory (DFT) combined with quantum chemical calculations to determine the first-order hyperpolarizability.

Keywords: Vibrational spectra; Fourier Transform infrared and FT-Raman spectra; DFT calculation, first-order hyperpolarizability

I. INTRODUCTION

1-Naphthol and derivatives thereof can also be used for the preparation of chiral ligands as contemplated by the present disclosure. Yet further naphthol derivatives are known in the art and are within the capacity of a skilled technician. 1-naphthol has been frequently used in chemical industries, e.g., in production of dyes, plastics, synthetic rubber, plant protecting formulations, etc. The toxicity of 1-naphthol is considered similar to that of naphthalene and carbaryl. Due to the presence of a hydroxyl group in its molecular structure, 1-naphthol solubility in water as well as its mobility in natural aquifers is enhanced. Biological monitoring is the best way for assessing exposure to organic contaminants and involves the measurement of a biomarker of exposure (usually the contaminant or a metabolite) in human blood, urine or biological tissues. So, fast, accurate and sensitive analytical methods are necessary for the examination of human exposure. 1-naphthol is an urinary metabolite of both naphthalene and carbaryl. As the biological half-live of carbaryl is on the order of days, 1-naphthol is an urinary biomarker of exposure to carbaryl indicative only of recent exposure.

Accurate vibrational assignment for aromatic and another conjugated system is necessary for characterization of materials. Assignment for complex systems can be proposed on the basis of frequency agreement between the computed harmonics and the observed fundamentals. Quantum chemical computational methods have proven to be an essential tool for interpreting and predicting vibrational spectra [1-2]. A significant advance in this area was made by scaled quantum mechanical (SQM) force field method [3-6]. In the SQM approach the systematic errors of the computed harmonic force field were corrected by a few scale factors which were found to be well transferable between chemically related molecules [2,7-9].

Recent spectroscopic studies on these materials have been motivated because the vibrational spectra are very useful for the understanding of specific biological process and in the analysis of relatively complex systems. In the present study, we extend a probing into the application of the B3LYP/6-31G* (small basis set) and 3LYP/6-311+G** (large basis set) based on SQM method [2] to vibrational analysis and

conformational stability of 1-Naphthol. The main difficulty in such investigation is that the vibrational spectra of these compounds have not been completely analyzed until now and generally only rough assignments are available. The geometrical parameters of the most optimized geometry obtained via energy calculations were used for the DFT calculations. The infrared and Raman intensities were also predicted. Based on these calculations, the simulated FT-IR and FT-Raman spectra were obtained. The observed and the simulated spectra agrees well.

II. EXPERIMENTAL DETAILS

The fine polycrystalline samples of 1-Naphthol were obtained from the Lancaster chemical company, UK, and used as such for the spectral measurements. The room temperature Fourier transform infrared spectra of the title compounds were measured in the 4000-400 cm^{-1} region at a resolution $\pm$ 1 cm^{-1} using KBr pellets on Perkin-Elmer RX1 FT-IR spectrophotometer equipped with He-Ne laser source, KBr beam splitter and LiTaO3 detector. Boxcar apodisation was used for the 250 averaged interferograms collected for both the samples and background. The FT-Raman spectra of 1-Naphthol were recorded on a BRUKERIFS-66V model interferometer equipped with an FRA106 and a FT-Raman accessory. The spectra were recorded in the 3500-100 cm^{-1} stokes region using the 1064 nm line of a Nd:YAG laser for the excitation operating at 200 mW power. The reported wave numbers are believed to be accurate within $\pm$ 1 cm^{-1}.

III. COMPUTATIONAL DETAILS

The calculation of the vibrational frequencies is essential and also useful for the vibrational assignments of the spectra. Quantum chemical calculations for 1-Naphthol was performed with the Gaussian 98 W program [10] using the Becke 3-Lee-Yang-Parr (B3LYP) functional [11,12] supplemented with the standard B3LYP/6–31G* (small basis set) and 3LYP/6–311+G** (large basis set) for the Cartesian representation of the theoretical force constants have been computed at the fully optimized geometry by assuming Cs point group symmetry. Scaling of the force field was performed according to the SQM procedure [13,14] using selective (multiple) scaling in the natural internal coordinate representation [15,16]. Transformations of the force field and the subsequent normal coordinate analysis including the least squares refinement of the scaling factors, calculation of total energy distribution (TED) and IR and Raman intensities were done on a PC with the MOLVIB program (Version V7.0-G77) written by Sundius [17,18].

The TED elements provide a measure of each internal coordinates contribution to the normal coordinate. For the plots of simulated IR and Raman spectra, pure Lorentzian band shapes were used with a bandwidth of 10 cm^{-1}. The prediction of Raman intensities was carried out by following the procedure outlined below. The Raman activities calculated by the Gaussian 98 W program and adjusted during scaling procedure with MOLVIB were converted to relative Raman intensities using the following relationship derived from the basic theory of Raman scattering [19-21].

$$I_i = \frac{f(v_o - v_i)^4 S_i}{v_i[1 - \exp(-hcv_i/kT)]}$$

where v_o is the exciting frequency (in cm^{-1} units), v_i the vibrational wavenumber of the i^{th} normal mode, h, c and k are the universal constants and f is the suitably chosen common scaling factor for all the peak intensities.

IV. ESSENTIALS OF NONLINEAR OPTICS RELATED TO β

The nonlinear response of an isolated molecule in an electric field $E_i(\omega)$ can be represented as a Taylor expansion of the total dipole moment μ_t induced by the field:

$$\mu_t = \mu_0 + \alpha_{ij} E_i + \beta_{ijk} E_i E_j + \ldots$$

Where α is linear polarizability, μ_0 the permanent dipole moment and β_{ijk} are the first-order hyperpolarizability tensor components.

The components of first-order hyperpolarizability can be determined using the relation

$$\beta_i = \beta_{iii} + \frac{1}{3}\sum_{i \neq j}(\beta_{ijj} + \beta_{jij} + \beta_{jji})$$

Using the x, y and z components the magnitude of the total static dipole moment (μ), isotropic

polarizability (α_0), first-order hyperpolarizability (β_{total}) tensor, can be calculated by the following equations:

$$\mu_1^0 = (\mu_x^2 + \mu_y^2 + \mu_z^2)^{1/2}$$

$$\beta_{tot} = (\beta_x^2 + \beta_y^2)^{1/2}$$

The complete equation for calculating the first-order hyperpolarizability from Gaussian 98 W output is given as follows [10]:

$$\beta_{tot} = [(\beta_{xxx} + \beta_{xyy} + \beta_{xzz})^2 + (\beta_{yyy} + \beta_{yzz} + \beta_{yxx})^2 + (\beta_{zzz} + \beta_{zxx} + \beta_{zyy})^2]$$

The β components of GAUSSIAN 98 W output are reported in atomic units, the calculated values have to be converted into electrostatic units (1 a.u = 8.3693 $\times$ 10^{-33} esu).

Before calculating the hyperpolarizability for the in-vestigated compound, the optimization has been carried out in the UHF (unrestricted open-shell Hartree-Fock) level. Molecular geometries were fully optimized by Berny's optimization algorithm using redun-dant internal coordinates. All optimized structures were confirmed to be minimum energy conformations.

An optimization is complete when it has converged. i.e., when it has reached a minimum on the potential energy surface, thereby predicting the equilibrium structures of the molecules. This criterion is very important in geometry optimization. The inclusion of d polarization and double zeta function in the split valence basis set is expected to produce a marked improvement in the calculated geometry [22]. At the optimized structure, no imaginary frequency modes were obtained proving that a true minimum on the potential energy surface was found. The electric dipole moment and dispersion free first-order hyperpolarizibility were calculated using finite field method. The finite field method offers a straight forward approach to the calcula-tion of hyperpolarizabilities [23]. All the calculations were carried out at the DFT level using the three-parameter hybrid density functional B3LYP and a 3-21 G (d, p) basis set.

V. RESULTS AND DISCUSSION

A. *Molecular Geometry*

The optimized molecular structure of 1-Naphthol was shown in Fig. 1. The global minimum energy obtained by the DFT structure optimization was presented in Table 1. The optimized geometrical parameters obtained by the large basis set calculation were presented in Table 2.

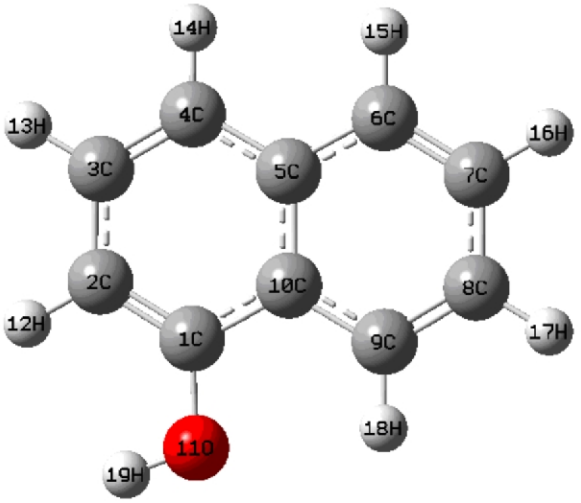

Fig. 1. Optimized molecular structure of 1-Naphthol

Table 1. Total energies of 1-Naphthol, Calculated at DFT (B3LYP)/6-31G* and (B3LYP)/6-311+G level**

Method	Energies (Hartrees)
6-31G*	–461.084753
6-311+G**	–461.109185

Detailed description of vibrational modes can be given by means of normal coordinate analysis (NCA). For this purpose, the full set of 72 standard internal coordinates containing 21 redundancies were defined as given in Table 3. From these, a non-redundant set of local symmetry coordinates were constructed by suitable linear combinations of internal coordinates following the recommendations of Fogarasi et. al [15, 16] are summarized in Table 4. The theoretically calculated DFT force fields were transformed in this later set of vibrational coordinates and used in all subsequent calculations.

Table 2. Optimized geometrical parameters of 1-Naphthol obtained by B3LYP/ 6-311+G density functional calculations**

Bond length	Value (Å)	Bond angle	Value (Å)	Dihedral angle	Value (Å)
C2-C1	1.379	C3-C2-C1	120.157	C4-C3-C2-C1	– 0.013
C3-C2	1.414	C4-C3-C2	120.797	C5-C4-C3-C2	0.022
C4-C3	1.375	C5-C4-C3	120.255	C6-C5-C4-C3	– 179.976
C5-C4	1.421	C6-C5-C4	122.131	C7-C6-C5-C4	– 179.955
C6-C5	1.420	C7-C6-C5	121.089	C8-C7-C6-C5	0.048
C7-C6	1.376	C8-C7-C6	120.320	C9-C8-C7-C6	– 0.092
C8-C7	1.415	C9-C8-C7	120.296	C10-C9-C8-C7	0.054
C9-C8	1.377	C10-C9-C8	120468	O11-C1-C2-C3	179.945
C10-C9	1.418	O11-C1-C2	122.792	H12-C2-C3-C4	179.953
O11-C1	1.368	H12-C2-C3	119.938	H13-C3-C4-C5	– 179.963
H12-C2	1.088	H13-C3-C4	120.253	H14-C4-C5-C6	0.0186
H13-C3	1.086	H14-C4-C5	119.064	H15-C6-C7-C8	– 179.981
H14-C4	1.086	H15-C6-C7	120.364	H16-C7-C8-C9	179.952
H15-C6	1.087	H16-C7-C8	119.674	H17-C8-C9-C10	– 179.985
H16-C7	1.086	H17-C8-C9	119.985	H18-C9-C10-C1	0.086
H17-C8	1.086	H18-C9-C10	118.791	H19-O11-C1-C2	– 0.096
H18-C9	1.084	H19-O11-C1	108.727		
H19-O11	0.969				

*for numbering of atom refer Fig. 1

B. Analysis of Vibrations Spectra

The 51 normal modes of 1-Naphthol are distributed among the symmetry species as $\Gamma_{3N-6} = 35\,A'$ (in-plane) $+ 16\,A''$ (out-of-plane), and in agreement with C_s symmetry. All the vibrations were active both in Raman scattering and infrared absorption. In the Raman spectrum the in-plane vibrations (A') give rise to polarized bands while the out-of-plane ones (A'') to depolarized band. The TED were reported in Table 5.

For visual comparison, the observed and simulated FT-IR and FT-Raman spectra of 1-Naphthol are produced in a common frequency scales in Fig. 2 & Fig. 3. Root mean square (RMS) values of frequencies were obtained in the study using the following expression,

Table 3. Definition of internal coordinates of 1-Naphthol

No (i)	Symbol	Type	Definition
Streching			
1 - 7	r_i	C-H	C2-H11, C3-H13, C4-H14, C6-H15, C7-H16, C8-H17, C9-H18
8	q_i	C-O	C1-O11
9	Q_i	O-H	O11-H19
10-20	R_i	C-C	C1-C2, C2-C3, C3-C4, C4-C5, C5-C6, C6-C7, C7-C8, C8-C9, C9-C10, C10-C1, C10-C5
Bending			
21-34	β_i	C-C-H	C1-C2-H12, C3-C2-H12, C2-C3-H13. C4-C3-H13, C3-C4-H14, C5-C4-H14, C5-C6-H15, C7-C6-H15, C6-C7-H16, C8-C7-H16, C7-C8-H17, C9-C8-H17, C8-C9-H18, C10-C9-H18.
35-36	θ_i	C-C-O	C10-C1-O11, C2-C1-O11
37	ϕ_i	C-O-H	C1-O11-H19
38-43	α_i	bring 1	C1-C2-C3, C2-C3-C4, C3-C4-C5, C4-C5-C10, C5-C10-C5, C10-C1-C2
44-49	α_i	bring 2	C5-C6-C7, C6-C7-C8, C7-C8-C9, C8-C9-C10, C9-C10-C5, C10-C5-C6
Out-of-plane bending			
50-56	ω_i	ω C-H	H12-C2-C1-C3, H13-C3-C2-C4, H14-C4-C3-C5, H15-C6-C5-C7, H16-C7-C6-C8, H17-C8-C7-C9, H18-C9-C8-C10.
57	ω_i	ωC-O	O11-C1-C10-C2
Torison			
58-63	τ_i	tring 1	C1-C2-C3-C4, C2-C3-C4-C5, C3-C4-C5-C10, C4-C5-C10-C1, C5-C10-C1-C2, C10-C1-C2-C3
64-69	τ_i	tring 2	C5-C6-C7-C8, C6-C7-C8-C9, C7-C8-C9-C10, C8-C9-C10-C5, C9-C10-C5-C6, C10-C5-C6-C7
70	τ_i	τO-H	C2 (C10)-C1-O11-H19
71-72	τ_i	Butterfly	C4-C5-C10-C9, C6-C5-C10-C1

*for numbering of atom refer Fig. 1

Table 4. Definiton of local symmetry coordinates and the value corresponding scale factors used to correct the force fields for 1-Naphthol

No.(i)	Symbol[a]	Definition[b]
1-7	C-H	r1, r2, r3, r4, r5, r6, r7
8	C-O	q8
9	O-H	Q9
10-20	C-C	R10, R11, R12, R13, R14, R15, R16, R17, R18, R19, R20
21-27	C-C-H	(β 21 - β 22) /√2, (β 23 - β 24) /√2, (β 25 - β 26) /√2 (β 27 - β 28) /√2, (β 29 - β 30) /√2 , (β 31 - β 32) /√2 , (β 33 - β 34) /√2
28	C-C-O	(θ 35 - θ 36) /√2
29	C-O-H	ϕ 37
30	bring 1	$(\alpha 38 - \alpha 39 + \alpha 40 - \alpha 41 + \alpha 42 - \alpha 43)/\sqrt{6}$
31	bring 1	$(2\alpha 38 - \alpha 39 - \alpha 40 + 2\alpha 41 - \alpha 42 - \alpha 43)\sqrt{12}$
32	bring 1	$(\alpha 39 - \alpha 40 + \alpha 42 - \alpha 43)/2$
33	bring 2	{(α44 – α45 + α46 – α47 + α48 – α49)/
34	bring 2	$(2\alpha 44 - \alpha 45 - \alpha 46 + 2\alpha 47 - \alpha 48 - \alpha 49)\sqrt{12}$
35	bring 2	$(\alpha 45 - \alpha 46 + \alpha 48 - \alpha 49)/2$
36-42	ω C-H	ω 50, ω 51, ω 52, ω 53, ω 54, ω 55, ω 56
43	ω C-O	ω 57
44	tring 1	$(\tau 58 - \tau 59 + \tau 60 - \tau 61 + \tau 62 - \tau 63)\sqrt{6}$
45	tring 1	$(\tau 58 - \tau 60 + \tau 61 - \tau 63)/2$
46	tring 1	$(-\tau 58 + 2\tau 59 - \tau 60 - \tau 61 + 2tau62 - \tau 63)\sqrt{12}$
47	tring 2	$(\tau 64 - \tau 65 + \tau 66 - \tau 67 + \tau 68 - \tau 69)\sqrt{6}$
48	tring 2	$(\tau 64 - \tau 65 + \tau 66 - \tau 67)\sqrt{2}$
49	tring 2	$(-\tau 64 + 2\tau 65 - \tau 66 - \tau 67 + 2tau68 - \tau 69)\sqrt{12}$
50	tO-H	t70
51	Butterfly	$(\tau 71 - \tau 72)/\sqrt{2}$

[a]These symbols are used for description of the normal modes by TED in Table 5.

[b]The internal coordinates used here are defined in Table 3.

Table 5. Detailed assignments of fundamental vibrations of 1-Naphthol by normal mode analysis based on SQM force field calculation

No.	Symmetry species Cs	Observed frequency (cm^{-1})			Calculated frequency (cm^{-1}) with B3LYP/6-311+G** force field			TED (%) among type of internal coordinates[c]
		Infrared	Raman	Unscaled	Scaled	IR^a A_i	Raman[b] I_i	
1	A′	3781		4129	3754	46.960	149.807	OH (100)
2	A′	3258		3549	3227	8.568	128.455	CH (99)
3	A′			3526	3206	20.078	329.074	CH (99)
4	A′			3524	3204	39.605	86.932	CH (99)
5	A′	3222		3510	3191	20.519	126.357	CH (99)
6	A′	3218		3505	3187	4.776	58.963	CH (99)
7	A′			3495	3178	1.212	39.227	CH (99)
8	A′	3198		3483	3167	20.719	106.842	CH (99)
9	A′	1705	1681	1857	1689	12.219	3.569	CC (66), bCH (13), bring 1 (9), bring 2 (8)
10	A′			1823	1658	28.033	0.697	CC (68), bCH (23)
11	A′	1652		1799	1636	51.772	47.257	CC (69), bCH (13), bring 1 (8), bring 2 (6)
12	A′	1588	1583	1730	1573	13.244	0.730	CC (57), bCH (32)
13	A′	1529	1519	1666	1515	7.486	14.639	bCH (44), CC (41)
14	A′	1519		1655	1505	7.114	51.206	bCH (59), CC (33)
15	A′	1462	1461	1592	1448	18.458	2.200	bCH (59), CC (25), bring 1 (7), CO (6)
16	A′	1443		1571	1429	45.380	96.795	CC (78), bCH (12)
17	A′	1420		1547	1407	13.142	55.089	CC (79), bCH (12)
18	A′	1332	1312	1450	1319	78.985	5.138	bCH (36), CO (27), CC (21), bring 1 (15)
19	A″	1294	1281	1410	1282	25.568	2.207	bCH (52), CC (28), bring 1 (8), CO (6)
20	A′	1281	1271	1395	1269	36.671	4.786	CC (33), bOH (28), bCH (25), bring 2 (12)
21	A′	1245	1242	1356	1233	30.830	6.080	CC (48), bCH (31), bOH (19)
22	A′	1208	1209	1316	1197	3.895	3.187	bCH (76), CC (14)
23	A′	1198		1305	1187	14.717	1.073	bCH (59), CC (35), bOH (5)
24	A′	1187	1184	1293	1176	9.480	8.844	bCH (52), CC (33), bring 1 (8), bOH (6)

No.	Symmetry species Cs	Observed frequency (cm^{-1})			Calculated frequency (cm^{-1}) with B3LYP/6-311+G** force field			TED (%) among type of internal coordinates[c]
		Infrared	Raman	Unscaled	Scaled	IR^a A_i	Raman[b] I_i	
25	A′	1121	1148	1222	1111	15.005	7.658	CC (45), bCH (27), bring 2 (17), CO (8)
26	A′	1081	1086	1178	1071	39.447	6.243	CC (37), bring 2 (19), bCH (16), CO (10), bring 1 (8)
27	A′	1059	1045	1153	1049	15.865	7.558	CC (74), bCH (14)
28	A″	1001		1091	992	0.002	0.103	gCH (87), tring 2 (13)
29	A″	973		1060	964	1.786	0.044	g CH (90)
30	A″	964	960	1050	955	0.027	0.027	gCH (92), tring 1 (6)
31	A′	899		980	891	10.449	3.571	bring 1 (34), bring 2 (33), CC (20), CO (7)
32	A″	896	877	976	888	1.298	4.247	gCH (75), tring 2 (14), tring 1 (10)
33	A″	862	861	939	854	0.002	1.367	gCH (81), tring 1 (11), gCO (7)
34	A″	810		883	803	41.362	2.603	gCH (40), tring 1 (31), tring 2 (20), gCO (9)
35	A′	808		881	801	6.361	0.558	bring 1 (40), bring 2 (33), CC (23)
36	A″	796	790	867	789	54.610	1.294	gCH (59), tring 2 (16), tring 1 (15), gCO (6)
37	A″	752	772	819	745	1.880	5.893	gCH (74), tring 2 (19), tring 1 (7)
38	A′	733	716	798	726	3.145	29.302	CC (48), bring 2 (31), bring 1 (8), CO (8)
39	A′	652	630	710	646	1.071	29.302	tring 2 (33), gCO (26), tring 1 (25), gCH (14)
40	A′	590	580	643	585	3.438	1.666	bring 2 (50), bring 1 (24), CC (16)
41	A″	590	575	643	585	1.185	8.756	tring 1 (43), gCH (19), tring 2 (14), tCC (12), gCO (12)
42	A′	538	540	586	533	4.871	4.995	bring 1 (34), bring 2 (30), bCO (19), CC (13)
43	A′	491	485	535	487	0.846	5.765	bring 1 (59), bring 2 (24), CC (11)
44	A″	483		526	479	0.389	0.344	tring 1 (42), tring 2 (40), gCH (15)
45	A′	474	467	517	470	0.581	5.884	bCO (37), CC (25), bring 1 (19), bring 2 (14)
46	A″	437		476	433	0.395	1.787	tring 2 (56), gCH (16), tCC (10), gCO (9), tring 1 (5)
47	A″	371		404	368	113.069	5.174	tOH (84), tring 2 (10)
48	A′	286	283	312	284	6.294	1.346	bCO (38), bring 2 (25), bring 1 (21), CC (14)

No.	Symmetry species Cs	Observed frequency (cm^{-1})			Calculated frequency (cm^{-1}) with B3LYP/6-311+G** force field			TED (%) among type of internal coordinates[c]
		Infrared	Raman	Unscaled	Scaled	IR^a A_i	Raman[b] I_i	
49	A″	267		291	265	4.465	1.014	tring 1 (45), tring 2 (21), gCH (15), tCC (11), gCO (7)
50	A″	179	171	195	178	4.019	0.026	tCC (28), tring 2 (25), tring 1 (25), gCH (16), gCO (6)
51	A″	144		157	143	0.457	2.428	tring 1 (60), tring 2 (31), gCH (7)

Abbreviations used: b, bending; g, wagging; t, torsion;

[a]Relative absorption intensities normalized with highest peak absorption

[b]Relative Raman intensities calculated by Eq.1 and normalized to 100.

[c]For the notations used see Table 4.

$$RMS = \sqrt{\frac{1}{n-1}\sum_{n-1}^{1}(U_1^{calc} - U_1^{exp})^2}$$

The RMS error of the observed and calculated frequencies (unscaled / B3LYP/6 – 311 + G^{**}) of 1-Naphthol was found to be 107 cm^{-1}. This is quite obvious; since the frequencies calculated on the basis of quantum mechanical force fields usually differ appreciably from observed frequencies. This is partly due to the neglect of anharmonicity and partly due to the approximate nature of the quantum mechanical methods. In order to reduce the overall deviation between the unscaled and observed fundamental frequencies, scale factors were applied in the normal coordinate analysis and the subsequent least square fit refinement algorithm resulted into a very close agreement between the observed fundamentals and the scaled frequencies. Refinement of the scaling factors applied in this study achieved a weighted mean

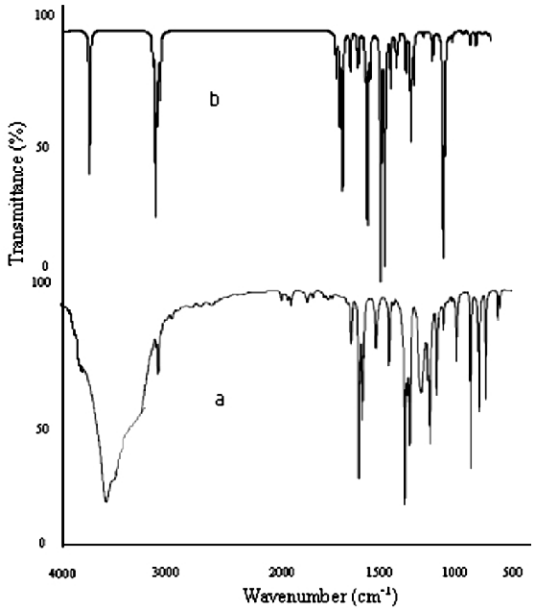

Fig. 2 FT-IR spectra of 1-Naphthol.
(a) Observed (b) Calculated with
B3LYP/6 – 311 + G^{**}

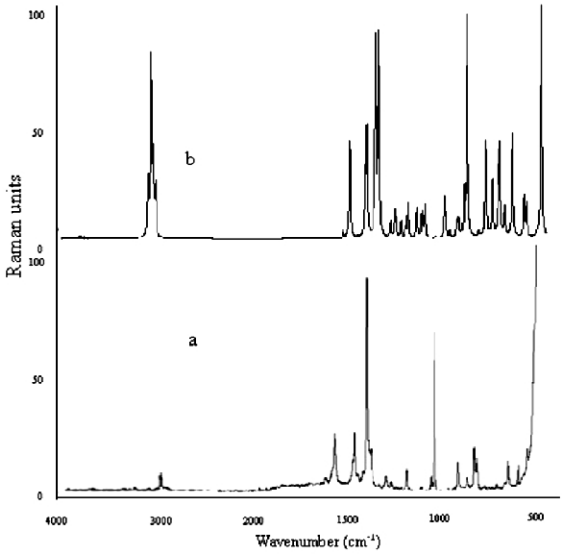

Fig. 3 FT-Raman spectra of 1-Naphthol.
(a) Observed (b) Calculated with
B3LYP/6 – 311 + G^{**}

deviation of 9 cm^{-1} between the experimental and scaled frequencies of the title compound.

C-C vibrations

The bands between 1407, 1636 and 1658 cm^{-1} are assigned to C-C stretching modes [24]. In the present study, the carbon stretching vibrations of the title compound have been observed at 1420, 1652 cm^{-1} in the FT-IR and 1583 cm^{-1} in FT-Raman spectrum and are presented in Table 5. These assignments are in good agreement with literature [25,26]. In present investigation, the C-C mode mixes with C-H in-plane bending vibrations.

C-H vibrations

The presence of hetro-aromatic-type structure is best recognized by the presence of C-H stretching vibrations [27] near 3200 cm^{-1}. Aromatic compounds commonly exhibit multiple weak bands in the region 3100-3000 cm^{-1} due to aromatic C-H stretching vibrations. The bands due to C-H in-plane ring bending vibration interacting with C-C stretching vibration are observed as a number of m-w intensity sharp bands in the region 1300-1000 cm^{-1}. C-H out-of-plane bending vibrations are strongly coupled vibrations and occur in the region 900-667 cm^{-1}. Accordingly, in the present study the C-H vibrations of the title compounds are occured at 3227, 3206, 3204, 3191, 3187, 3178 and 3167 cm^{-1} for 1-Naphthol.

C-O vibrations

The non-linearity of hydrogen bond in 1-Naphthol have an impact over the carbonyl group frequency. The interaction of carbonyl group with the other group present in the system does not produce such a drastic and characteristic changes in the frequency of C O stretch. The carbonyl stretching frequency is very sensitive to the factors that disturb the nature of the carbonyl group and its precise frequency is characteristic of the type of the carbonyl compound being studied. Particularly detailed correlations have been made for the carbonyl bond stretching frequency.The carbonyl stretching frequency has been most extensively studied by infrared spectroscopy. This multiply bonded group is highly polar ($> Cd^{\delta+} = Od^{\delta-}$) and therefore gives rise to an intense infrared absorption band. The carbon-oxygen dou-ble bond is formed by the $pp_{\pi} - pp_{\pi}$ bonding between carbon and oxygen. Because of the different electro-negativities of carbon and oxygen atoms, the bonding electrons are not equally distributed between the two atoms. The following two resonance forms contribute to the bonding of the car-bonyl group $> C = O \leftrightarrow C + - O^{-}$. The lone pair of electrons on oxygen also determines the nature of the carbonyl group. The position of the C = O stretching vibration is very sensi-tive to various factors such as the physical state, electronic effects by substituents, ring strains, etc. [24]. Consideration of these factors provides further information about the environ-ment of the C=O group. The carbonyl stretching generally occurs as a strong absorption in the region from 1448, 1319, 1282, 1111, 1071, 891 cm^{-1}. This portion of the infrared spectrum is most useful because the position of the carbonyl absorption is quite sensitive to substitution effects and the geometry of the molecule.

OH vibrations

The precise positions of O-H band are dependent on the strength of hydrogen bond. The O-H stretching appears at 3800-3500 cm^{-1} in the inter-molecular hydrogen bonded systems. The observed peaks in this region are sharp and strong. The title compounds in this study showed a very strong absorption peak at 3754 cm^{-1} which are due to the O-H stretching vibrations.

C-O stretching and O-H bending vibrations

Two bands arising from C-O stretching and O-H bending appear in the spectra of carboxylic acids near 1210-1320 and 1400-1440 cm^{-1}, respectively. Both these bands involve some interaction between C-O stretching and in-plane C-O-H bending. The more intense band near 1280-1315 cm^{-1} for dimers is generally referred to as CO stretching band and it usually occurs as a doublet in the spectra of long-chain fatty acids. One of the characteristic bands in the spectra of dimeric carboxylic acid arises from the out-of-plane bending of the hydrogen bonded OH. It appears near 1071 cm^{-1} and is characteristically broad with medium intensity [24].

Ring vibrations

Several ring modes are affected by the substitution in the aro-matic ring. In the present study, the bands absorbed at 1689, 1636, 1448, 1319, 1282 cm^{-1} and 891, 801, 585, 487 cm^{-1} have been designated to ring in-plane and out-of-plane bending modes, respectively. For most of the remaining ring

vibrations, the overall agreement is satisfactory. Small changes in frequencies observed for these modes are due to the changes in force constants/reduced mass ratio resulting mainly due to the extent of mixing between ring and substituent group.

C. Hyperpolarizability calculations

The first-order hyperpolarizibility (β_{ijk}) of the novel molecular system of 1-Naphthol is calculated using 3-21 G (d,p) basis set based on finite field approach. Hyperpolarizibility is a third rank tensor that can be described by a $3 \times 3 \times 3$ matrix. It strongly depends on the method and basis set used. The 27 components of 3D matrix can be reduced to 10 components due to Kleinman symmetry [28]. The calculated first-order hyperpolarizability (btotal) of 1-Naphthol is $1.1070 \times 10 - 30^{-30}$ esu, which is nearly six times that of urea (0.1947×10^{-30} esu). The calculated dipole moment (μ) and first-order hyperpolarizibility (β) are shown in Table 6. The theoretical calculation seems to be more helpful in determination of particular compo-nents of β tensor than in establishing the real values of β. Domination of particular components indicates on a substantial delocalization of charges in those directions. It is noticed that in β_{yyy} (which is the principal dipole moment axis and it is parallel to the charge transfer axis) direction, the biggest values of hyperpolarizability are noticed and subsequently delocalization of electron cloud is more in that direction. The higher dipole moment values are associated, in general, with even larger projection of β_{total} quantities. The electric dipoles may enhance, oppose or at least bring the dipoles out of the required net alignment necessary for NLO properties such as β_{total} total values. The connection between the electric dipole mo-ments of an organic molecule having donor-acceptor substituent and first hyperpolarizability is widely recog-nized in the literature [29]. The maximum β was due to the behavior of non-zero μ value. One of the conclusions obtained from this work is that non-zero μ value may enable the finding of a non-zero β value. Of course Hartee-Fock calculations depend on the mathematical method and basis set used for a polyatomic molecule.

Table 6. The dipole moment (m) and First-order hyperpolarizibility (b) of 1-Naphthol derived from dft calculations

β_{xxx}	– 30.036823
β_{xxy}	30.0437602
β_{xyy}	– 13.7476317
β_{yyy}	– 161.8470719
β_{zxx}	0.0600745
β_{xyz}	0.1220257
β_{zyy}	– 0.6719205
β_{xzz}	0.4894769
β_{yzz}	0.0155964
β_{zzz}	– 0.0025623
b_{total}	1.1070
μ_x	0.4960665
μ_y	0.1145269
μ_z	0.0019529
μ	0.5091

Dipole moment (μ) in Debye, hyperpolarizibility $\beta\ (-2\omega; \omega, \omega)\ 10^{-30}$ esu.

V. CONCLUSION

In this work, the SQM force field method based on DFT calculations at the B3LYP/$6-311+G^{**}$ level have been carried out to analyze the vibrational frequencies of 1-Naphthol. Refinement of the scaling factors applied in this study achieved a weighted RMS deviation of 9 cm^{-1} between the experimental and scaled frequencies. This close agreement established between the experimental and scaled frequencies obtained using large basis set ($6-311+G^{**}$) calculations has proved to be more reliable and accurate than the calculations using lower basis sets. The first-order hyperpolarizibility (β_{ijk}) of the novel molecular system of 1-Naphthol is calculated using 3-21 G (d,p) basis set based on finite field approach.

The calculated first-order hyperpolarizability (β_{total}) of 1-Naphthol is 1.1070 $\times$ 10^{-30} esu, which is nearly six times that of urea (0.1947 $\times$ 10^{-30} esu).

ACKNOWLEDGEMENT

The authors are thankful to the Sophisticated Analytical Instrumentation Facility (SAIF), IIT Madras, Chennai, for spectral measurements. Help rendered by S. Anbarasan, Spectroscopic Division, Photonics Research Foundation, Salem, in the calculation part highly acknowledged.

REFERENCES

[1] B.A. Hess Jr., J. Schaad, P. Carsky, R. Zahradnik, Chem. Rev. 86 (1986) 709.

[2] P. Pulay, X. Zhou, G. Fogarasi, in: R. Fausto (Ed.), NATO ASI Series, vol. C406, Kluwer, Dordrecht, 1993.

[3] C.E. Blom, C. Altona, Mol. Phys. 31 (1976) 1377.

[4] P. Pulay, G. Fogarasi, G. Pongor, J.E. Boggs, A. Vargha, J. Am. Chem. Soc. 105 (1983) 7037.

[5] G. Fogarasi, P. Pulay, in: J.R. Durig (Ed.), Vibrational Spectra and Structure, vol. 14, Elsevier, Amsterdam, 1985.

[6] G. Fogarasi, Spectrochim. Acta 53A (1997) 1211.

[7] G. Pongor, P. Pulay, G. Fogarasi, J.E. Boggs, J. Am. Chem. Soc. 106 (1984) 2765.

[8] G.R. De Mare, Y.N. Panchenko, C.W. Bock, J. Phys. Chem. 98 (1994) 1416.

[9] Y. Yamakita, M. Tasumi, J. Phys. Chem. 99 (1995) 8524.

[10] M.J. Frisch, G.W. Trucks, H.B. Schlega, G.E. Scuseria, M.A. Robb, J.R. Cheesman, V.G. Zakrzewski, J.A. Montgomery Jr., R.E. Stratmann, J.C. Burant, S. Dapprich, J.M. Millam, A.D. Daniels, K.N. Kudin, M.C. Strain, O. Farkas, J. Tomasi, V. Barone, M. Cossi, R. Cammi, B. Mennucci, C. Pomelli, C. Adamo, S. Clifford, J. Ochterski, G.A. Petersson, P.Y. Ayala, Q. Cui, K. Morokuma, N. Roga, P. Salvador, J.J. Dannenberg, D.K. Malick, A.D. Rabuck, K. Rahavachari, J.B. Foresman, J. Cioslowski, J.V. Ortiz, A.G. Baboul, B.B. Stefanov, G. Liu, A. Liashenko, P. Piskorz, I. Komaromi, R. Gomperts, R.L. Martin, D.J. Fox, T. Keith, M.A. Al-Laham, C.Y. Penng, A. Nanayakkara, M. Challa-Combe, P.M.W. Gill, B. Johnson, W. Chen, M.W. Wong, J.L. Andres, C. Gonzalez, M. Head-Gordon, E.S. Replogle and J.A. Pople, Gaussian 98, Revision A 11.4, Gaussian Inc., Pittsburgh, PA (2002).

[11] A.D. Becke, J.Chem. Phys.98 (1993) 5648.

[12] C. Lee, W. Yang, R.G. Parr, Phys. Rev. B.37 (1998) 785.

[13] P. Pulay, G. Fogarasi, G. Pongor, J.E. Boggs, A. Vargha, J.Am. Chem. Soc. 105 (1983) 7037.

[14] G. Rauhut, P. Pulay, J. Phys. Chem. 99 (1995) 3093.

[15] G. Fogarasi and P. Pulay In: J.R. Durig, Editor, Vibrational Spectra and Structure vol. 14, Elsevier, Amsterdam (1985), p. 125 (Chapter 3).

[16] G. Fogarasi, X. Xhov, P.W. Taylor and P. Pulay, J. Am. Chem. Soc. 114 (1992), p. 8191.

[17] T. Sundius. J. Mol. Struct. 218 (1990) 321.

[18] (a) T. Sundius, Vib. Spectrosc. 29 (2002) 89-95. (b) MOLVIB (v.7.0), Calculation of harmonic force fields and vibrational modes of molecules, QCPE Program No. 807, 2002.

[19] P.L. Polavarapu, J. Phys. Chem. 94 (1990) 8106.

[20] G. Keresztury, S. Holly, J. Varga, G. Besenyei, A.V. Wang, J.R. Durig, Spectrochim. Acta 49A (1993) 2007.

[21] G. Keresztury, in: J.M. Chalmers and P.R. Griffiths (Eds), Handbook of Vibrational Spectroscopy vol.1, John Wiley & Sons Ltd. (2002), p. 71.

[22] A.D. Becke, J.Chem. Phys. 98 (1993) 5648.

[23] H.D. Cohen, C.C.J. Roothan, J. Chem. Phys. 435 (1965) S34.

[24] D.N. Sathyanarayana, Vibrational Spectroscopy-Theory and Applica-tions, second ed., New Age International (P) Limited Publishers, New Delhi, 2004.

[25] George Socrates, Infrared and Raman Characteristic Group Frequencies -Tables and Charts (third ed.), John Wiley & Sons, Chichester (2001).

[26] V. Krishna kumar, R. John Xavier, Indian J. Pure Appl. Phys. 41 (2003) 95.

[27] B. Lakshmaiah, G. Ramana Rao, J. Raman Spectrosc. 20 (1989) 439.

[28] D.A. Kleinman, Phys. Rev. 126 (1962) 1977.

[29] P.N. Prasad, D.J. Williams, Introduction to Nonlinear Optical Effects in Molecules and Polymers, Wiley, New York, 1991.